NUREG/CR-6675

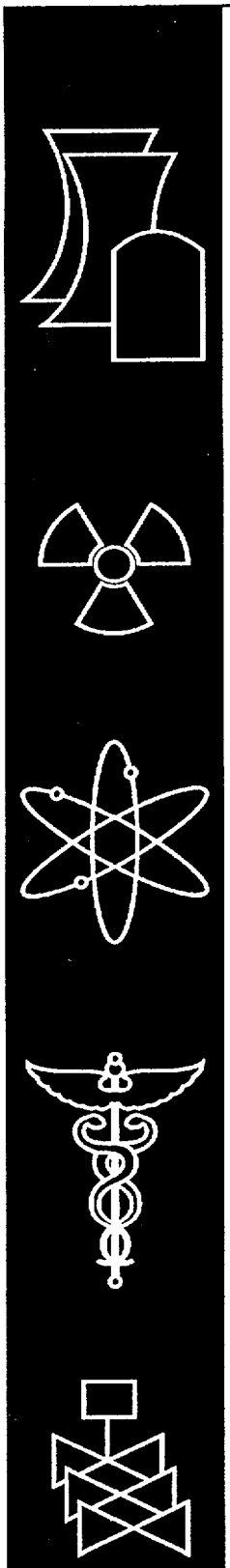

Interaction of Zinc Vapor With Zircaloy and the Effect of Zinc Vapor on the Mechanical Properties of Zircaloy

National Institute of Standards and Technology

U.S. Nuclear Regulatory Commission
Office of Nuclear Regulatory Research
Washington, DC 20555-0001

AVAILABILITY OF REFERENCE MATERIALS IN NRC PUBLICATIONS

NRC Reference Material

As of November 1999, you may electronically access NUREG-series publications and other NRC records at NRC's Public Electronic Reading Room at www.nrc.gov/NRC/ADAMS/index.html. Publicly released records include, to name a few, NUREG-series publications; *Federal Register* notices; applicant, licensee, and vendor documents and correspondence; NRC correspondence and internal memoranda; bulletins and information notices; inspection and investigative reports; licensee event reports; and Commission papers and their attachments.

NRC publications in the NUREG series, NRC regulations, and *Title 10, Energy*, in the Code of *Federal Regulations* may also be purchased from one of these two sources.

1. The Superintendent of Documents
   U.S. Government Printing Office
   P. O. Box 37082
   Washington, DC 20402–9328
   www.access.gpo.gov/su_docs
   202–512–1800
2. The National Technical Information Service
   Springfield, VA 22161–0002
   www.ntis.gov
   1–800–553–6847 or, locally, 703–605–6000

A single copy of each NRC draft report for comment is available free, to the extent of supply, upon written request as follows:

Address: Office of the Chief Information Officer,
Reproduction and Distribution
Services Section
U.S. Nuclear Regulatory Commission
Washington, DC 20555-0001
E-mail: DISTRIBUTION@nrc.gov
Facsimile: 301–415–2289

Some publications in the NUREG series that are posted at NRC's Web site address www.nrc.gov/NRC/NUREGS/indexnum.html are updated regularly and may differ from the last printed version.

Non-NRC Reference Material

Documents available from public and special technical libraries include all open literature items, such as books, journal articles, and transactions, *Federal Register* notices, Federal and State legislation, and congressional reports. Such documents as theses, dissertations, foreign reports and translations, and non-NRC conference proceedings may be purchased from their sponsoring organization.

Copies of industry codes and standards used in a substantive manner in the NRC regulatory process are maintained at—

The NRC Technical Library
Two White Flint North
11545 Rockville Pike
Rockville, MD 20852–2738

These standards are available in the library for reference use by the public. Codes and standards are usually copyrighted and may be purchased from the originating organization or, if they are American National Standards, from—

American National Standards Institute
11 West 42nd Street
New York, NY 10036–8002
www.ansi.org
212–642–4900

The NUREG series comprises (1) technical and administrative reports and books prepared by the staff (NUREG–XXXX) or agency contractors (NUREG/CR–XXXX), (2) proceedings of conferences (NUREG/CP–XXXX), (3) reports resulting from international agreements (NUREG/IA–XXXX), (4) brochures (NUREG/BR–XXXX), and (5) compilations of legal decisions and orders of the Commission and Atomic and Safety Licensing Boards and of Directors' decisions under Section 2.206 of NRC's regulations (NUREG–0750).

NUREG/CR-6675

Interaction of Zinc Vapor with Zircaloy and the Effect of Zinc Vapor on the Mechanical Properties of Zircaloy

Manuscript Completed: May 2000
Date Published: June 2000

Prepared by
R.J. Schaefer, R.J. Fields, M.E. Williams

National Institute of Standards and Technology
Gaithersburg, MD 20899

C. Santos, Jr., NRC Project Manager

Prepared for
Division of Engineering Technology
Office of Nuclear Regulatory Research
U.S. Nuclear Regulatory Commission
Washington, DC 20555-0001
NRC Job Code Y6212

ABSTRACT

Spent fuel rods removed from reactor cores are loaded under water into steel casks, which are then removed from the water, vacuum dried, and welded closed for dry storage. In some cases, the inside of the steel casks has been coated with zinc paint to prevent corrosion during the under-water phase of this process, and concern has arisen that the zinc could react with the Zircaloy-4 cladding of the spent fuel, possibly leading to decreased mechanical strength. This project investigated the kinetics of the reaction between Zircaloy-4 and zinc vapor, and the mechanical properties of Zircaloy-4 which had been exposed to zinc vapor.

CONTENTS

Page

Abstract iii

Abbreviations vii

1 Introduction 1

2 Description of Previous Investigation 2

3 Objectives of Present Study 4

4 Experimental Procedure 6

4.1 Materials 6

4.1.1 Sample Materials 6

4.1.2 Zinc Vapor Source 6

4.2 Procedures 6

4.2.1 Sample Preparation 6

4.2.2 Heat Treatment 7

4.2.3 Temperature Calibration 7

4.2.4 Sample Quenching 8

4.2.5 Choice of Heat Treatment Temperatures 8

4.3 Microstructural Characterization 8

4.3.1 Metallography 8

4.3.2 Energy Dispersive Spectrometry 8

4.4 Mechanical Testing 8

4.4.1 Design of Samples and Grips 9

4.4.2 Testing Arrangement 9

5 Experimental Results 11

5.1 Reaction Products 11

5.2 Mechanical Tests 16

6 Discussion 20

6.1 Reaction Rates 20

6.2 Mechanical Behavior 21

7 Conclusions 26

8 References 27

Figures

1 Grips used for slow strain rate tensile tests 10

2 Zircaloy-4 samples reacted with zinc at 300 °C 11

3 Zircaloy-4 samples reacted with zinc at 350 °C 12

4 Zircaloy-4 samples reacted with zinc at 400°C 13

5 Oxide layer on end-of-life Zircaloy-4 tubing 14

6 Intermetallic layers formed in some regions under the oxide coating, after exposure for 10 days at 350 °C 14

7 Fracture surface of Sample MT1, showing cleavage fracture in the intermetallic layers and ductile fracture in the untransformed material 16

8 Inner surface of Sample MT1, showing fracture of intermetallic phases 16

9 Effect of exposure conditions on the onset of plasticity as detected by the C-bend test at room temperature 23

10 Effect of exposure condition on the slow strain rate ultimate tensile strength of Zircaloy tubes tested at the temperatures indicated 24

11 Effect of exposure conditions on the ductility of Zircaloy tubes tested in slow strain rate tension at the temperatures shown 24

12 Assuming that the IMC layer is not load bearing, the UTS of the remaining Zircaloy is recalculated using the measured thickness of intermetallic and its stoichiometry 25

Tables

1 Low-Temperature Reaction Tests with Bare Zircaloy-4 4

2 Pre-exposure Conditions for Mechanical Test Samples 4

3 Reaction Tests with Oxide-Coated Zircaloy-4 5

4 Vapor Pressure of Zinc 7

5 C-Bend Test Results 18

6 Tensile Test Results 19

ABBREVIATIONS

DCSS	dry cask storage system
EDS	energy dispersive spectrometry
EOL	end of life
ISFSI	independent spent fuel storage installation
IMC	intermetallic compound
NIST	National Institute of Standards and Technology
NRC	U.S. Nuclear Regulatory Commission
PWR	pressurized water reactor
SEM	scanning electron microscopy
TREX	tube reduced extrusion
UTS	ultimate tensile strength

1 INTRODUCTION

The Nuclear Regulatory Commission (NRC) has under consideration, and is anticipating license applications for the construction, operation, and decommissioning of fuel-cycle facilities. These applications include, but are not limited to, those for licenses and license extensions of Independent Spent Fuel Storage Installations (ISFSI) and for approval of storage cask designs. Safety and environmental reviews of the applications related to these license extensions must be performed and considered as part of the licensing process. The design and performance of an ISFSI and the criteria used to assess compliance with regulatory requirements may be governed by the behavior and performance characteristics of the materials in the ISFSI over extended periods.

When spent fuel rods are removed from a reactor core, they are placed in a water pool for approximately five years to radioactively "cool." They are then loaded under water into a steel storage container called a cask: the loading of a cask may take up to a week. When the loading is completed, the cask is removed from the water, vacuum dried, back-filled with an inert gas, and the top is sealed by welding. During vacuum drying, the maximum internal temperature may reach 570 °C, and during normal dry storage the internal temperature is expected to equilibrate at approximately 350 °C and subsequently decay slowly.

During the underwater spent fuel loading, it was found that corrosion of the steel cask produced radioactive iron particles that contaminated the storage pool filters. To prevent this corrosion, in recent years the inside of the casks has been coated with zinc paint. However, the presence of zinc within the system creates the potential for reaction with the Zircaloy-4 tubes that contain the fuel. During dry storage, it is possible that zinc vapor may evaporate from the paint, deposit on the Zircaloy cladding of the fuel rods, and react with or diffuse into the Zircaloy. The concern is that during a storage period which could be as much as 100 years, these reactions might lead to cracking of the cladding if the reaction layer thicknesses or stresses within the cladding become large. This cracking in turn might allow escape of nuclear material from the rods. For this reason, the NRC previously supported a study (Ref. 1) by NIST of "Reactions of Zinc Vapor with Zircaloy." That study made some preliminary observations of the reaction products formed on the surface of Zircaloy when exposed to zinc vapor. The present study adds to the information obtained in that work, and extends the work to an investigation of the effect of the reaction products on the mechanical properties of Zircaloy.

2 DESCRIPTION OF PREVIOUS INVESTIGATION

Layer growth in which the layer thickness increases as a function of time presumably would require diffusion of either zinc or zirconium through this alloyed layer. If the layer growth is diffusion-controlled, the layer thickness at constant temperature should increase proportional to the square root of the time, and in such a case it should be possible to use short-term tests to predict long-time layer thicknesses. Diffusion rates are expected to increase exponentially with temperature. Thus, if x is the layer thickness and t is the time during which diffusion-controlled growth of this layer proceeds, one expects in a simple diffusion-controlled process that

$$x^2 t^{-1} = K\exp(-Q/RT) \qquad (1)$$

where T is the absolute temperature, K is a constant independent of temperature, R is the gas constant (8.314 joule/mole-degree Kelvin), and Q is an activation energy. The constants Q and K in this equation can be evaluated by measuring the layer thicknesses, x, obtained during times, t, at several different temperatures. One can then, in principle, predict the layer thicknesses expected during 100 years at lower temperatures from measurements made for much shorter times at higher temperatures.

This procedure has the potential of providing predictions for the behavior at long times and low temperatures, based on experiments carried out for short times at high temperatures. However, in order for this procedure to be valid, a single activation energy must hold true throughout the entire temperature range. A temperature range must therefore be selected in which the crystallographic phases present are the same as those present at the temperature for which the predictions are to be made.

Zircaloy-4 is a dilute alloy of zirconium containing 1.5 wt % tin, 0.2 wt % iron, and 0.1 wt % chromium. The published zirconium-zinc binary phase diagram indicated a eutectoid reaction at approximately 750 °C, and the experiments were therefore carried out below this temperature.

Zircaloy-4 samples were reacted with zinc vapor in quartz ampoules under vacuum. Because the reactions were carried out at temperatures above the melting point of pure zinc, high-purity brass was used in these ampoules as the source of zinc. At temperatures near 700 °C, the brass becomes rapidly dezincified since zinc has a much higher vapor pressure than copper.

The thickness of the reaction layer formed in these experiments at 650 °C, 670 °C, and 700 °C was measured, and an activation energy of 143 kJ/mole was derived. Due to uncertainties in the measurements, it was estimated that the activation energy could lie in the rather broad range from 100 kJ/mole to 180 kJ/mole. The measured composition of the reacted material corresponded roughly to layers consisting of the intermetallic compounds Zn_2Zr and ZnZr.

Using these results in Equation (1), one estimates that the layer thickness formed in 100 years at 350 °C would lie in the range 0.7 μm to 9 μm, with 2.5 μm being the penetration that corresponds to the central activation energy value of 143 kJ/mole.

However, an additional experiment was carried out in which a Zircaloy specimen was encapsulated under vacuum with chips of pure zinc and heated at 350 °C for 169 days. This temperature was below the melting point (419.5 °C) of zinc, so it was not necessary to use brass as the source of zinc vapor. In this experiment, the reaction did not form a uniform layer on the surface, but did form a large number of bead-like reaction products that cover almost the entire surface to a thickness of about 25 μm. The composition of the reacted material corresponded to Zn_3Zr. This thickness is much larger than that which would be predicted from extrapolation of the results found from the exposure tests between 650 °C and 700 °C, and it suggested that the reaction mechanism at the lower temperature was significantly different from that prevailing between 650 °C and 700 °C. More low-temperature exposure experiments were therefore needed to understand the probable progression of reactions in casks during prolonged storage.

3 OBJECTIVES OF PRESENT STUDY

The formation of intermetallic compounds, which in most cases are brittle, on the surface of Zircaloy samples exposed to zinc gives rise to concern that the strength of the Zircaloy tubing could be degraded. A program was therefore initiated to make preliminary measurements of:

1. The interaction of Zircaloy at low temperatures (300°C to 400°C) with vapor from high-purity zinc.
2. The mechanical properties of Zircaloy which had been exposed to zinc vapor.
3. The effect of an oxide layer on the Zircaloy, typical of an end-of-use condition, on the reaction of Zircaloy with zinc vapor.

The program also sought to estimate, on the basis of the measurements of interactions in the 300°C to 400 °C range, the probable thickness of the reaction product on Zircaloy tubing over the lifetime of a dry cask storage system.

A series of exposures was formulated to provide a rapid but representative set of measurements. Table 1 lists the low-temperature reaction tests with bare Zircaloy-4. Table 2 lists the pre-exposure conditions for mechanical test samples (2 samples were exposed at each of the indicated conditions). Table 3 lists the reaction tests with oxide-coated Zircaloy-4.

Table 1 Low-Temperature Reaction Tests with Bare Zircaloy-4

	300 °C	350 °C	400 °C
10 days	X	X	X
30 days	X	X	X
90 days	X	X	X

Table 2 Pre-exposure Conditions for Mechanical Test Samples

	Room temp.	300 °C	350 °C	400 °C	650 °C
no exposure	9 samples				
30 days					2 samples
90 days			2 samples	2 samples	
>90 days*		2 samples	2 samples	1 sample	

*Samples prepared for possible follow-on experiments.

Table 3 Reaction Tests with Oxide-Coated Zircaloy-4		
	350 °C	650 °C
10 days	X	X
90 days	X	X

4 EXPERIMENTAL PROCEDURE

4.1 Materials

4.1.1 Sample Materials

All samples used in this study were provided by McDermott Technology, Inc.* (formerly Babcock & Wilcox R&D) in Lynchburg, Virginia.

Diffusion experiments were performed on three types of non-radioactive samples: (1) Zircaloy-4 tube reduced extrusion (TREX) samples, (2) Zircaloy-4 tubing in the as-received condition (lot #3Me13-8), and Zircaloy-4 tubing with oxidation layer.

The Zircaloy-4 TREX material had a 6.35 cm outside diameter and a wall thickness of 1.27 cm. Pieces cut from this material were used for the low temperature reaction studies.

The Zircaloy-4 as-received tubing was used for the mechanical properties tests. It was already stress relieved through annealing at 500 °C by the supplier. This tubing has dimensions of 11 mm outside diameter and a wall thickness of 0.75 mm.

The Zircaloy-4 EOL tubing with a 100 μm thick oxide layer on the inside and outside of the tube was used to study the effects which an oxide layer may have on the Zn-Zircaloy reactions. The EOL tubing dimensions are 11.2 mm outside diameter and a 0.76 mm wall thickness. This oxide layer was produced by flowing pure oxygen over the tube surface at 600 °C for 100 h.

4.1.2 Zinc Vapor Source

The zinc vapor source used for this study was special high purity zinc (99.999+%). The pieces of zinc were cut into cubes with sides approximately 4 mm in length with a diamond saw. The zinc pieces were etched in Nital etchant for 10 min, then cleaned in an ultrasonic bath with acetone and then ethyl alcohol. All pieces were weighed and stored in a desiccator.

4.2 Procedures

4.2.1 Sample Preparation

The Zircaloy-4 TREX samples were sliced from bulk material with a diamond saw. All of these samples were cut to approximately the same dimensions, 12 mm long, 3 mm wide and 1.5 mm thick. The surfaces were ground, finishing with wet 600 grit SiC paper, and then polished with a 6 μm diamond suspension. The samples were then cleaned with acetone and ethanol and air-dried. Samples were encapsulated in a quartz tube under vacuum of 1.33×10^{-5} Pa. The samples were annealed at approximately 700 °C for six days in order to relieve any stresses introduced by the extrusion process and sample preparation. After air cooling the tube containing the annealed samples was broken and each sample was polished to 1/4 μm finish, cleaned and then individually encapsulated with the high purity zinc with ultra high purity helium.

The tubing samples were cut to 40 mm lengths. For the mechanical properties tests, a 14.5 mm ±0.1mm (2σ uncertainty) gage

section with a reduced wall thickness of 0.375 mm ±.025 mm (2σ uncertainty) was then machined in the middle of the as-received tubing. The EOL tubing had a 3 mm wide strip ground (400 grit SiC and then polished to a 1/4 μm finish) lengthwise to expose a region of bare Zircaloy-4. Both the as–received tubing (pre-annealed at 500 °C) and the end of life (EOL) tubing were cleaned with acetone and ethyl alcohol and encapsulated with zinc.

At the highest experimental temperature of 650 °C, the zinc vapor pressure is 3.59 kPa The vapor pressure of zinc was calculated using equation 2, where P is in mm Hg and the temperature T is in Kelvins (Ref. 2).

$$\log_{10} P = \frac{-0.05223(a)}{T} + b \qquad (2)$$

For liquid zinc in the temperature range between 600 °C and 985 °C, the values of the constants are a=118,000 and b=8.108. For solid zinc in the temperature range of 250 °C to the melting point 419.5 °C, the constant values are a=133,000 and b=9.2. Table 4 lists the zinc vapor pressure at the heat treatment temperatures.

Table 4 Vapor Pressure of Zinc

Temperature (°C)	Pressure (Pa)
650	3.59×10^3
400	10.1
350	1.5
300	0.16

4.2.2 Heat Treatment

A 5 cm inside diameter vertical tube furnace was used for the heat treatments. A nickel-chromium cylindrical container, 8.25 cm tall with a 3.75 cm inside diameter, with lid, was placed in the middle of the furnace hot zone and allowed to equilibrate at the furnace temperature. This minimized temperature differences within the container. The furnace tube above and below the container was packed with firebrick to prevent convection currents in the tube. The encapsulated sample was placed inside the Nichrome container and was monitored by a sheathed type K (chromel-alumel) thermocouple placed through the lid to within 5 mm of the sample. This thermocouple was connected to a large external aluminum isothermal plate that served as the cold junction reference. This external panel was then connected to a temperature data acquisition board in a computer. The furnace temperature was maintained with a separate type K thermocouple connected to a temperature controller.

4.2.3 Temperature Calibration

The furnace was calibrated using a pure element encapsulated in quartz. The furnace temperature is set approximately 10 °C below the element's melting point. Once the furnace is equilibrated, the encapsulated standard is placed in the Nichrome container. The furnace temperature is raised by one degree and the standard is removed and visually inspected for melting and then placed back in the Nichrome container and the furnace is then allowed to re-equilibrate. This process is repeated until the standard melts. The temperature of the thermocouple monitoring the standard is recorded and then all other thermocouples are placed in that furnace one at a time and their temperatures

are recorded. The thermocouples were Inconel-sheathed type K with the thermocouple junction tip grounded to the sheath. Using three different furnaces set at the melting points of lead, zinc, and aluminum (327 °C, 419 °C, and 660 °C respectively), each thermocouple had a three point calibration. All thermocouples were corrected using these results.

4.2.4 Sample Quenching

At the end of the diffusion anneal the samples were quenched in water at room temperature. The sample was immersed in the water and then the quartz tube was broken using a hammer. The time from removal of the sample from the furnace until the quartz tube is broken underwater was approximately 5 to 10 seconds.

4.2.5 Choice of Heat Treatment Temperatures

The experiments were performed with Zircaloy-4 TREX, and Zircaloy-4 tubing in as-received and EOL conditions, encapsulated with high purity zinc in helium at 650 °C, 400 °C, 350 °C and 300 °C. The 650 °C temperature allowed a common test temperature between the previous high temperature tests and this low temperature study. The choice of low temperatures for these diffusion experiments was based on the temperature profile of a sealed cask which contains zinc.

4.3 Microstructural Characterization

4.3.1 Metallography

All of the samples were cut in cross section and mounted in epoxy resin for optical metallography. The samples were then ground with 400 and 600 grit wet SiC papers and then polished starting with 15 μm diamond suspension and finishing with ¼ μm diamond suspension. The grain size measurement of the Zircaloy-4 tubing and Zircaloy-4 TREX materials was performed using the circular intercept method, ASTM standard test method E112-96, on a ¼ μm diamond polished sample, etched with a solution of hydrofluoric acid, nitric acid and water. The measured grain sizes of the as-received tubing material and Zircaloy-4 TREX were found to be approximately 2 μm and 10 μm, respectively. After grain size measurements, all of the samples were repolished to a ¼ μm surface finish to remove the effects of the chemical etch.

4.3.2 Energy Dispersive Spectrometry

Each sample was examined with a scanning electron microscope (SEM). Using Energy Dispersive Spectrometry (EDS) with elemental standards for zinc, zirconium, tin, iron, and chromium, a compositional line scan was done on each sample. All line scans were preformed with an accelerating voltage of 20 kV, a probe current of 525 pA, and a 100 s acquisition time. The EDS composition profiles started at the edge of the sample and the electron beam was scanned toward the middle. The SEM electron beam resolution for EDS analysis is ≈1 μm and the line scan steps were varied from 0.5 μm to 1.5 μm. The results gave a composition profile and the penetration depth of the zinc diffusion reaction zone.

4.4 Mechanical testing

Two types of tests were performed on Zircaloy tubing: slow strain rate, uniaxial

tensile tests of tubes at 350 °C and 100 °C, and C-bend tests at room temperature. The rationale for these types of tests was based on the possibility that the Zircaloy may in some way be embrittled by exposure to zinc. If the tubes were severely embrittled, the room temperature C-bend test would reveal this fact. If, however, the zinc requires the presence of stress and elevated temperature to cause, for example, a grain boundary embrittlement by diffusion, the bend test might not detected it. In this case, the slow strain rate tests at elevated temperatures will be more likely to indicate some degradation in ductility or strength. The temperatures were chosen based on the range of temperatures that the tubes would see in storage. The slow strain rate (approximately 5.75 μstrain/s) was chosen so that some diffusion of Zn could occur and yet permit the tests to be completed in a timely fashion. Elevated temperature tests were done in He gas to simulate the storage conditions. All tests of exposed tubing were compared to results on as-received Zircaloy tubing that was never, at any time, exposed to zinc.

4.4.1 Design of Samples and Grips

The C-bend test of tubing was chosen for its simplicity. A circular ring of Zircaloy, 1 mm to 2 mm in length, was cut from the tube. A section of the ring was removed so that it resembled the letter "C". This was loaded in compression at the top and bottom of the "C" by two flat and parallel platens while recording the applied force and displacement of the platens until fracture or plastic collapse occurred. The samples and testing procedures met the requirements of ASTM Standard Test Method C1323-96.

The tensile testing of the tubes was complicated by the limited length of tubing that can be exposed to zinc. The longest specimen possible had a 14.5 mm ±0.1 mm reduced section gage length and 12.5 mm ±0.1 mm long grip section on each end. The reduced section had a nominal wall thickness of 0.375 mm ±0.025 mm, while the unreduced wall was 0.750 mm ±0.010 mm thick. All uncertainties in sample dimensions are 2 standard deviations. To hold these specimens during testing, a split ring collet grip was designed and fabricated. It consisted of a split tapered ring that fit tightly around the tube, with the taper fitting into a tapered socket. As the sample was loaded, the taper was drawn into the socket causing the split ring to tighten around the sample. Solid plugs were inserted only into the grip end regions to keep the thin walled Zircaloy tube from collapsing, wrinkling, or buckling. A photograph of these grips is shown in Figure 1.

4.4.2 Testing Arrangement

C-bend testing was carried out on a screw-driven compression testing machine at a free-running crosshead speed of 8.3 μm/s. These tests were performed at room temperature in laboratory air. Force and crosshead displacement were recorded until plastic collapse or fracture occurred.

Slow strain rate tensile tests were carried out on a screw-driven tensile testing machine at a free-running crosshead speed of 0.083 μm/s. This testing machine was equipped with a vacuum/environmental chamber and oven that was used to test the samples in gettered He gas at 100 °C and 350 °C. The

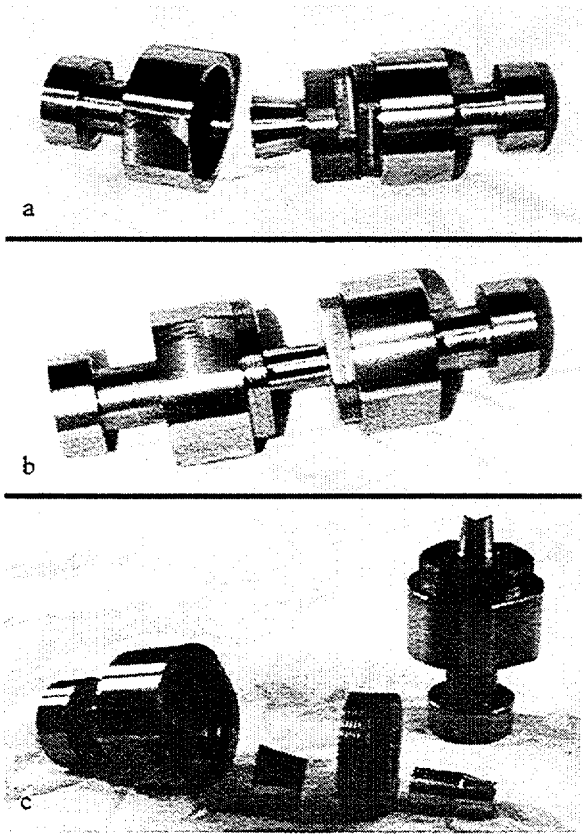

Figure 1 Grips used for slow strain rate tensile tests, showing a) grips with tapered collet, b) fully assembled system with Zircaloy-4 tubing sample, and c) disassembled system after failure of the sample by ductile fracture.

testing procedure usually consisted of mounting the sample in the grips described above. The grip/sample assembly was then mounted between pull rods in the chamber. The chamber was then evacuated to a pressure of about 1.3 mPa for about 15 min. At this point, gettered He was used to back fill the chamber until it reached atmospheric pressure. A slight overpressure was obtained by slowly bubbling the outflow through vacuum pump oil. The oven temperature was then raised at about 10 °C/min to the desired temperature. When thermal equilibrium had been established as indicated by thermocouples at the top and bottom of the sample being within 3 °C of each other, tensile testing was begun at the predetermined, slow rate. Force and cross head displacement were recorded during the test until fracture occurred. Force calibration in both the C-bend tests and tensile tests was made using proving rings traceable to NIST. Extension was calibrated using a dial gage that itself was calibrated using gage blocks traceable to NIST. After testing, the sample elongation and reduction in wall thickness were determined. Scanning electron microscopy was used to examine the fracture surface and determine the fracture mechanism.

5 EXPERIMENTAL RESULTS

5.1 Reaction Products

All samples were cut in cross section, mounted and polished to ¼ μm finish.

The exposure tests were planned based on the assumption that the reaction of zinc vapor with Zircaloy would produce a uniform reaction layer, with a growth rate proportional to the square root of time, and with a temperature dependence described by an Arrhenius relation. Such behavior would be describable by only two parameters, an activation energy and a diffusivity parameter, and would allow prediction of layer growth at long times. The results of the exposure tests, however, indicated a more complex behavior. In many cases the reaction product was nodular or irregular in cross section. The thicknesses cited are therefore only typical or illustrative values.

Reaction at 300 °C:

The formation of intermetallics was very slow at 300 °C and seemed to be limited by nucleation of the intermetallic phase. No intermetallics were detected at 10 days (sample ZR9) or 30 days (sample ZR13). At 90 days (sample ZR5), widely scattered nodules of Zn_3Zr were seen. These nodules had a maximum diameter of approximately 2 μm and covered approximately 10 % of the surface (Figure. 2).

Reaction at 350 °C:

The reaction at 350 °C (Figure 3) generally proceeded by the growth of nodules of Zn_3Zr. After 10 days (sample ZR7) the nodules had an average height of approximately 7 μm and occupied virtually all of the Zircaloy surface. Surprisingly, the 30 day sample (sample ZR10) showed less

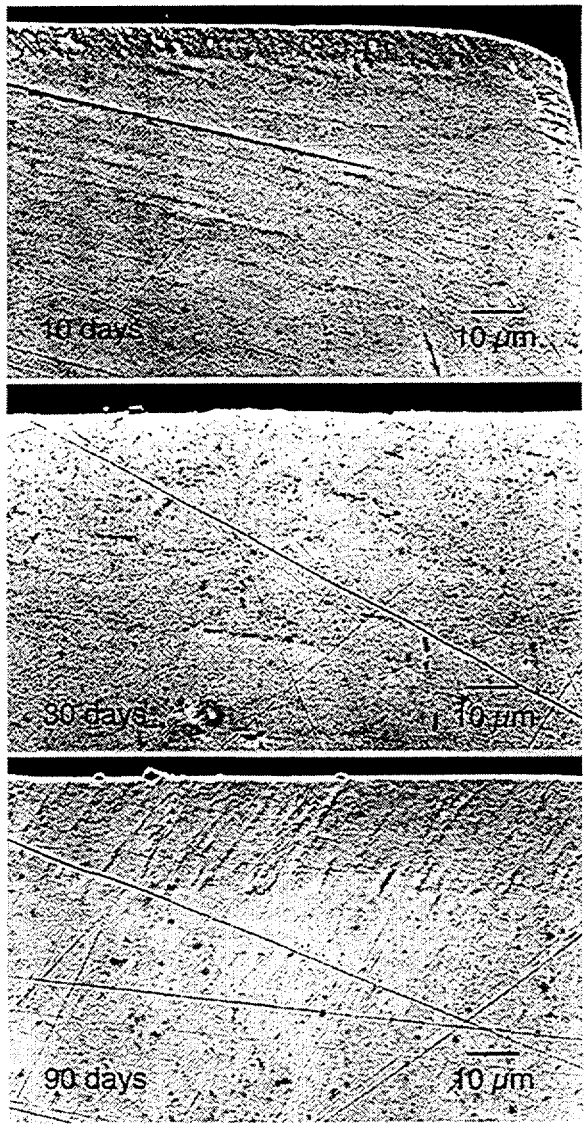

Figure 2 Zircaloy-4 samples reacted with zinc at 300 °C. Small nodules of Zn_3Zr were present only in the 90-day sample. No zinc was detected in the slightly rough-looking sub-surface layers seen in the 10 day and 30 day samples.

reaction than the 10 day sample, with large gaps of unreacted Zircaloy between small groups of extremely small intermetallic nodules. The 90 day sample (sample ZR12) showed a uniform layer of Zn_3Zr intermetallic approximately 70 μm to 80 μm thick. Two additional samples exposed at 350 °C were available from a previous study (1). A sample exposed for 15 days showed nodules of Zn_3Zr approximately 40 μm thick, while a sample exposed for 169 days showed Zn_3Zr nodules approximately 25 μm thick.

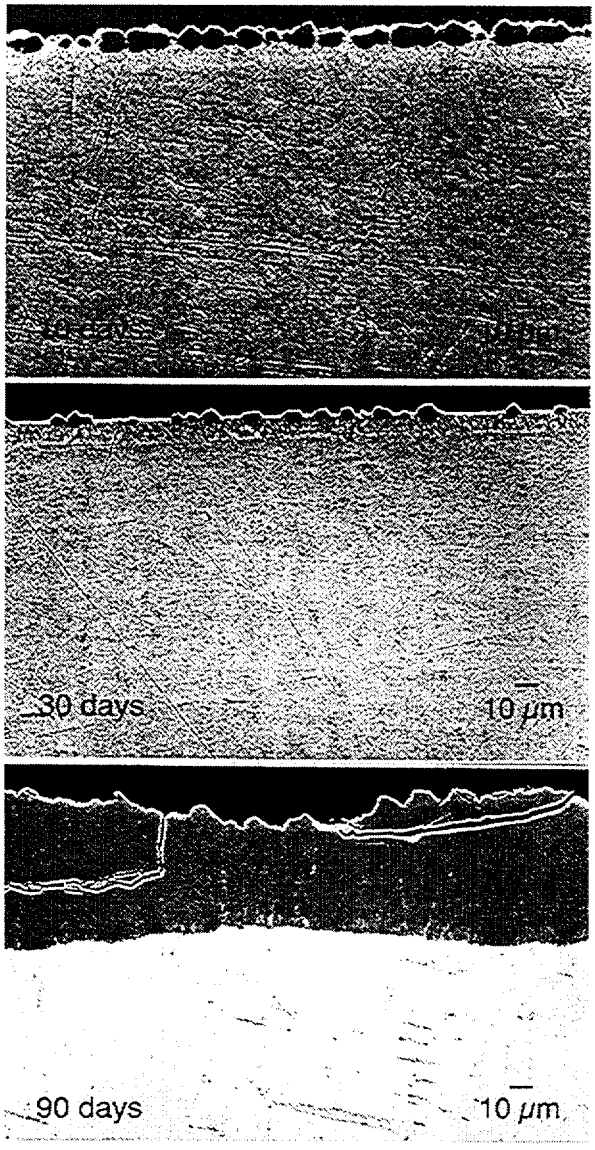

Figure 3 Zircaloy-4 samples reacted with zinc at 350 °C.

The reaction at 350 °C also was measured on the machined tubes on which the mechanical tests were carried out. Two of these were exposed at 350 °C for 90 days, and both showed a reaction layer of Zn_3Zr. On sample MT8, this layer was nodular and about 15 μm thick on the inside of the tube and 25 μm thick and more uniform on the outside of the tube. On sample MT9, under nominally identical conditions, the intermetallic had a layered structure 100 μm thick on the inside of the tube, with the outer half being very porous. The intermetallic layer was 40 μm thick and rather uniformly dense on the outside of the tube.

Reaction at 400 °C:

The samples reacted at 400 °C (Figure 4) showed startling differences. At 10 days (sample ZR6), nodules of intermetallic phases approximately 10 μm thick were observed, following a trend which might be expected from the 10 day samples at 300 °C and 350 °C. The nodules consisted of an outer layer of Zn_3Zr, with a possible layer of Zn_2Zr approximately 2 μm thick adjacent to the Zircaloy. However, at 30 days (sample ZR8) and 90 days (sample ZR11), the samples showed no trace of the nodular structure. Instead, very thick and uniform layers of intermetallic were present. At 30 days, these layers were approximately 450 μm thick, with the outer 380 μm consisting of Zn_6Zr and the remainder of Zn_3Zr. A similar structure was seen at 90 days, with the total thickness being 520 μm with the outer layer of Zn_6Zr having a thickness of 280 μm and the remainder being Zn_3Zr.

Machined tubes also were exposed at 400 °C. Sample MT14, exposed for 90 days, had a layer of Zn_3Zr approximately 60 μm thick on the inside and 50 μm thick on the outside. Sample MT6, exposed for 103 days, had similar layers of Zn_3Zr, 100 μm thick, with the outer half being extremely porous, on the inside and 75 μm thick on the outside.

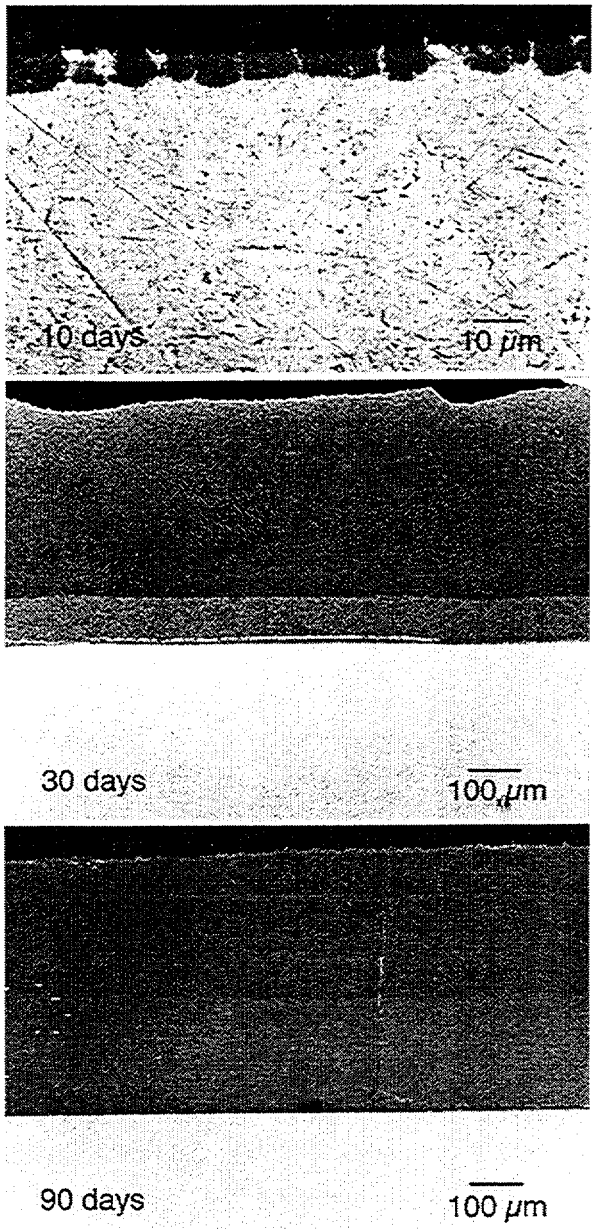

Figure 4 Zircaloy-4 samples reacted with zinc at 400 °C. Note that the magnification of the 10-day sample is greater than that of the 30-day and 90-day samples, and that the morphology of the intermetallic phases is different.

The growth of the reaction layer may in many cases have been limited by the supply of zinc. Consider the case of the mechanical test samples, 40 mm long with an outside diameter of 11 mm and a wall thickness of 0.75 mm. The surface area of such a tube is approximately 2600 mm^2. Covering the surface of this tube with a 1 μm layer of zinc would therefore require 2.6 mm^3, or 18.5 mg of zinc. Because the weight of zinc enclosed with the MT samples was typically 400 mg, it would be sufficient to cover the MT samples with a layer of Zn approximately 22 μm thick, or a layer of Zn_3Zr approximately 29 μm thick, or a somewhat thicker layer of a higher Zr compound. On this basis, it is probable that the thickness of the intermetallic layers on all of the mechanical test samples, except probably MT8, was limited by the supply of zinc, rather than by the time of exposure.

The TREX samples had a much smaller surface area, typically about 115 mm^2, and the amount of zinc enclosed with each of them was typically about 350 mg. To produce a 1 μm layer of zinc on one of these samples would require about 0.8 mg of zinc, so the 350 mg charge of zinc would be sufficient to produce a zinc layer approximately 440 μm thick, or a layer of Zn_3Zr approximately 580 μm thick. The thickness of the reaction layer would thus in general not be limited by the zinc supply on the TREX samples, except perhaps in the case of the samples exposed for 30 days and 90 days at 400 °C.

End-of Life tubing samples:

The unexposed EOL tubing samples (Figure 5) had a 100 μm thick oxide layer (ZrO_2) that had numerous fine cracks parallel to the metal surface and larger, less frequent cracks perpendicular to the surface. The interface with the Zircaloy tubing was not planar but had a scalloped morphology.

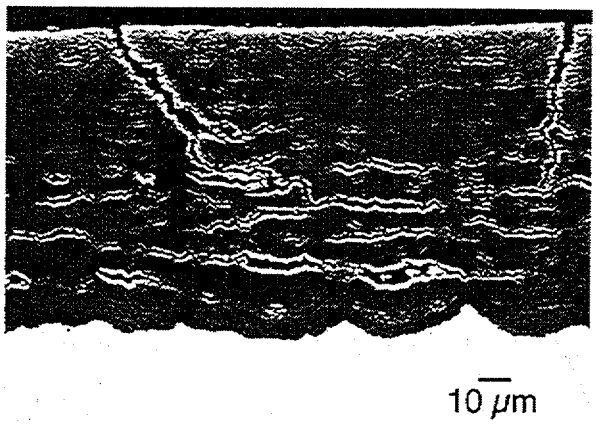

Figure 5 Oxide layer on end-of-life Zircaloy-4 tubing.

In the EOL tubing exposed to zinc vapor for 10 days at 350 °C (Figure 6), intermetallic phases formed in some regions in layers under the oxide at the tubing interface and had a scalloped shape accentuating the oxide-metal interface contours. The inner layer contained approximately 50 at. % Zr and may possibly be the ZnZr intermetallic. The second layer contained approximately 30 at. % Zr, corresponding to the Zn_2Zr intermetallic phase. However, in most regions no intermetallic layer was seen under these conditions. In the sample exposed at the same temperature for 90 days, no intermetallic phase was seen under the the oxide layer.

When the EOL tubing was removed from

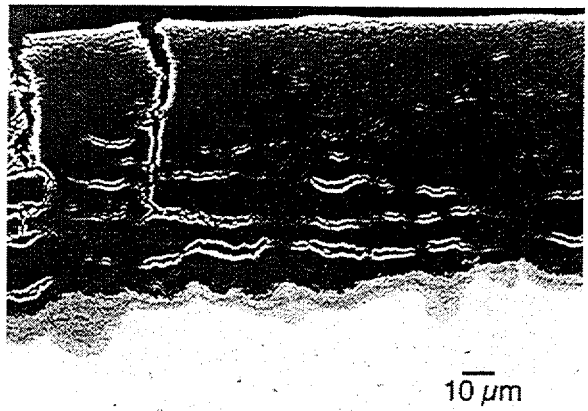

Figure 6 Intermetallic layers formed in some regions under the oxide coating, after exposure for 10 days at 350 °C.

the furnace, following exposure to zinc for 10 days at 650 °C, it was observed that the oxide layer near the ends of the tube and near the lengthwise strip of exposed Zircaloy had a loose flaky structure which crumbled away from the tubing. In a region where the oxide still adered to the tubing, a thin layer of intermetallic, varying in thickness from 5 μm to 20 μm, was present under the oxide. As in the case of the sample exposed at 350 °C, the intermetallic layer consisted of ZnZr and Zn_2Zr. In the regions where the oxide crumbled away from the tubing, a thick (170 μm) layer of intermetallic compound with a smooth interface with the underlying Zircaloy was present.This intermetallic consisted of a thick outer layer of Zn_3Zr, followed by a thin layer of Zn_2Zr approximately 10 μm thick and an innermost two-phase layer about 2 μm thick. In these regions, a very rough, spongy outer surface of this sample contained remnants of the oxide. The EOL tubing exposed to zinc for 90 days at 650 °C showed formation of a rather thin (about 15 μm) but uniform layer of intermetallic under the oxide.

Summary of Exposure Tests:

The intermetallic phases produced by the reaction between zinc vapor and Zircaloy, as revealed in this study, have distinctly different morphologies at low and high temperatures.

At low temperatures, the reaction product consists of isolated nodules of Zn_3Zr on the Zircaloy surface, generally characteristic of a process in which the intermetallic phase nucleates at only a limited number of sites, and then grows by diffusion of the zinc atoms along the surface of the Zircaloy. The size and spacing of these nodules did not appear to vary in a systematic way with the time of exposure, suggesting that the rates of nucleation and surface diffusion depended strongly on the condition of the Zircaloy sample surface. Although all samples received nominally the same surface preparation before the start of the exposure, factors such as surface oxidation, topography, and work hardening could well have varied enough to influence surface nucleation and diffusion processes. Because of the variability of the nodular growth reaction, it is not possible to develop an accurate model of the growth rates based on the current data.

At higher temperatures, a completely different type of reaction occured, characterized by formation of uniform layers of intermetallic phases. These layers grew much more rapidly than the nodules, with the result that all of the zinc within the ampoules was apparently consumed. The thickness of the intermetallic layers therefore probably was limited by the supply of zinc, rather than the reaction kinetics. Once the primary supply of zinc is exhausted, the intermetallic layers will tend to transform to the most zirconium-rich of the intermetallic phases. This process may account for the relatively greater thickness of the Zn_3Zr in the sample exposed for 90 days at 400 °C, compared to the thickness of the Zn_3Zr in the sample exposed for 30 days. As the intermetallic layers transform to more zirconium-rich phases, they will increase in thickness, for a fixed amount of zinc.

The change from the low temperature nodular growth to the high temperature layer growth appeared to be somewhat erratic: layer growth was seen in the 90-day sample at 350 °C but nodular growth was seen in all other 350 °C samples, and nodular growth was seen in the 10-day sample at 400 °C but layer growth was seen in the other two samples.

While the sample exposed at 350 °C for 169 days in the previous study (Ref. 1) showed an unexpectedly large reaction compared to that which would be predicted based on extrapolation of measurements carried out between 650 °C and 700 °C, the data measured in this study show reaction rates, especially at 400 °C, which are even more dramatically rapid. The source of zinc vapor in the high-temperature tests of the previous study was α-brass, as opposed to the pure zinc used in this study. The reaction rates in the previous study were therefore probably lower than they would have been if pure Zn had been used.

The oxide layer appeared to be rather effective at protecting the Zircaloy from attack by the zinc, at least in regions that

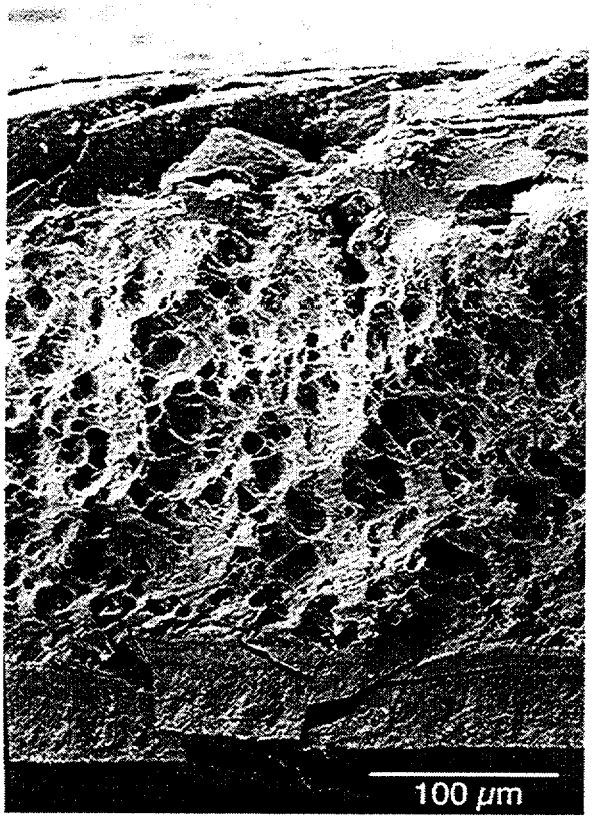

Figure 7 Fracture surface of sample MT1, showing cleavage fracture of the intermetallic layers and ductile fracture in the untransformed material.

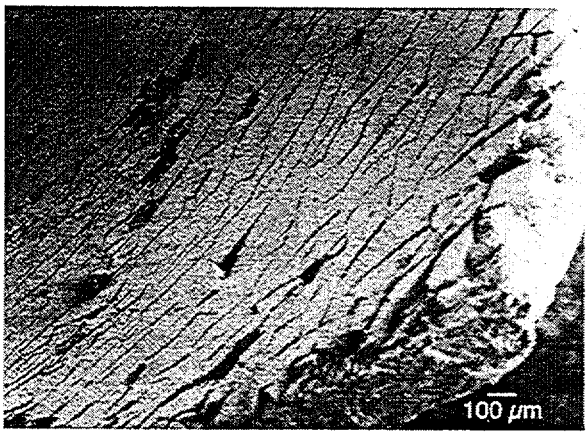

Figure 8 Inner surface of sample MT1, showing fracture of intermetallic phases.

were not close to a region of unprotected metal. Close to the regions where the oxide coating is broken, at 650 °C the oxide showed a tendency to crumble away from the tubing, and the formation of the intermetallic appeared quite rapid.

5.2 Mechanical Tests

The C-bend test samples all failed by plastic collapse. The load at the onset of plasticity and the specimen dimensions were used to calculate the outer fiber stress using the formula in ASTM C 1323. The results of these calculations are shown in Table 5. The uncertainty indicated by "±" in Table 5 represents one standard deviation.

The results of the slow strain rate tensile tests are given in Table 6. Tensile tests at room temperature indicated that the as-received tubes had an approximate yield strength of 302 MPa and an ultimate tensile strength (UTS) of about 347 MPa. This indicates that the material was typical of tubes in the cold-worked and stress-relieved condition. The tubes were not in the recrystallized condition. All but one of the fracture surfaces of the unexposed tubes were 100 % fibrous in nature, indicating completely ductile fracture. At 350 °C, there was a small region of intergranular fracture in one unexposed sample (not shown). This may have been an anomaly and did not significantly affect the overall ductile fracture behavior. The fracture surfaces of the exposed tubes consisted of 100% cleavage in the intermetallic layers and 100% fibrous fracture in the unreacted portion of the tube. It is clear from the fractographs (Figures 7 and 8) that the intermetallic was extremely brittle and cracked extensively during the deformation of the remaining unreacted Zircaloy. At the end of the tests, the intermetallic layers

formed at 650 °C had largely spalled off in the test at 100 °C, but were adherent at 350 °C. The layers formed at 350 °C and 400 °C were adherent at all test temperatures.

The presence of the intermetallic layers resulted in decreased load bearing capacity and a substantial decrease in the ductility, as measured by the strain-to-fracture, when compared to the unexposed tubes.

Estimate of Uncertainty

The uncertainty in the results arises from measurement uncertainty and the sample-to-sample variation. In the case of the C-ring bend tests, the two critical measurements are force at the onset of plasticity and the sample dimensions. The bias in these types of measurements is extremely small. The measurement uncertainty is dominated by the precision to which the recording instruments may be read. The force is known to within 1 N and the sample dimensions to within 25 μm. These uncertainties result in a one sigma uncertainty in the stress of about 28 MPa. The actually measured standard deviation in the stress for four nominally identical, unexposed samples was 21 MPa, so the uncertainty is dominated by the measurement uncertainty. The measured standard deviation on the exposed samples was somewhat larger than 28 MPa, so slight variations in exposure conditions may have resulted in a sample-to-sample variation that increased the uncertainty by as much as a factor of 1.5 in the worst case.

A similar estimate of uncertainty is carried out in what follows for the tensile tests on the Zircaloy tubes. The measurement uncertainty arises mainly from the measurement of maximum force and sample dimensions. The former is known to within 45 N and the latter to within 25 μm. These uncertainties result in a one sigma uncertainty in the UTS of 21 MPa and in the elongation-to-fracture of 0.4 % strain. The ranges of UTS and elongation values measured on nominally identical samples are in agreement with these uncertainties. For unexposed samples, the uncertainty is dominated by the measurement uncertainty rather than the sample-to-sample variation. The situation for the exposed samples is more complicated because only one sample was tested at each condition. This was done because of the extremely limited number of exposed samples and the need to uncover conditions of severe embrittlement rather than obtain statistical significance. Using the factor deduced for the effect of sample-to-sample variation on the uncertainty of the C-ring bend test results, the uncertainty in the tensile tests results for the exposed samples was estimated at 1.5 times the uncertainty of the unexposed samples.

Table 5 C-Bend Test Results		
Condition	Yield Strength in Bending (MPa)*	Failure Mode
No Exposure to Zn	690±21	Plastic Collapse
30 days at 650 °C	362±37	Plastic Collapse
90 days at 400 °C	528±32	Plastic Collapse
90 days at 350 °C	684±43	Plastic Collapse

*The uncertainty represents one standard deviation. See text for a discussion of the uncertainties in these values.

Table 6 Tensile Test Results					
Condition	Strain Rate (s^{-1})	Test Temp. (°C)	UTS‡ (MPa)	ϵ_f‡ (%)	Failure Mode
Unexposed A	$6x10^{-4}$	R.T.*	-	19.0±0.4	100 % Fibrous Load not recorded
Unexposed B	$6x10^{-4}$	R.T.*	694±21	19.5±0.4	100 % Fibrous
Unexposed C	$6x10^{-6}$ and $6x10^{-4}$†	350	478±21	24.3±0.4	99 % Fibrous 1 % Intergranular
Unexposed D	$6x10^{-6}$	350	358±21	-	Grip Slipped No Fracture
Unexposed E	$6x10^{-6}$	350	350±21	24.4±0.4	Grip Slipped, Reloaded 100 % Fibrous
Unexposed F	$6x10^{-6}$	100	582±21	18.6±0.4	100 % Fibrous
Unexposed G	$6x10^{-6}$	100	570±21	18.9±0.4	100 % Fibrous
Unexposed H	$6x10^{-6}$	350	352±21	22.6±0.4	100 % Fibrous
Unexposed I	$6x10^{-6}$	350	348±21	23.6±0.4	100 % Fibrous
Exposed to Zn 30 days at 650 °C	$6x10^{-6}$	350	214±32	11.3±0.6	100 % cleavage in intermetallic, 100% fibrous in remaining Zircaloy
Ditto	$6x10^{-6}$	100	352±32	16.6±0.6	Ditto
90 days at 400 C	$6x10^{-6}$	350	335±32	10.2±0.6	Ditto
103 days at 400 °C	$6x10^{-6}$	100	535±32	6.9±0.6	Ditto
90 days at 350 °C	$6x10^{-6}$	350	322±32	13.2±0.6	Ditto
Ditto	$6x10^{-6}$	100	516±32	7.2±0.6	Ditto

* Test run in laboratory air instead of the usual, gettered He gas.

† Test run slowly in gettered gas to just past yield point, followed by testing at a higher rate in vacuum to obtain UTS.

‡ The uncertainty represents one standard deviation. See text for a discussion of the uncertainties in these values.

6 DISCUSSION

6.1 Reaction Rates

In order to estimate the amount of reaction product which might form on a Zircaloy fuel rod due to reaction with zinc in the lifetime of a DCSS system, it is necessary to consider the system's thermal history and the kinetics of formation of the reaction product. Zircaloy fuel rods in a DCSS are subjected to a temperature which decreases slowly with time as the decay of radioactive species in the spent fuel proceeds. Figure 4-47 of Reference 3 shows the expected temperatures of the cladding, starting at approximately 3.5 years and extending to 40 years. Assuming an ambient temperature of 15 °C, the curve shown in this figure can be described well at short times (3.5 years to 8 years) by

$$T = 15 + 765.6\exp(-0.1285t) \qquad (3)$$

and at long times (8 years to 40 years) by

$$T = 15 + 287.5\exp(-0.02149t) \qquad (4)$$

where in both equations T is the temperature in °C and t is the time in years. The latter expression can be extrapolated to estimate the temperatures at times up to 100 years.

If the reaction product between Zircaloy and zinc is modeled as a uniform layer of intermetallic compound of fixed composition, a simple model of the thickening process can be derived. The growth rate of the layer will be limited by diffusion through the layer (either diffusion of Zr to the outside surface or diffusion of Zn to the inside surface), as described by

$$\frac{dh}{dt} = AD\frac{dC}{dx} \qquad (5)$$

where h is the thickness of the layer, D is the diffusion coefficient of the diffusing species, A is a constant, and dC/dx is the concentration gradient of the diffusing species in the layer. We can write

$$\frac{dC}{dx} = \frac{C_1 - C_2}{h} \qquad (6)$$

where C_1 is the concentration at the outside surface, set by the activity of the zinc vapor, and C_2 is the concentration at the inner surface of the layer, set by the equilibrium with the underlying zircaloy. Combining these equations and integrating yields

$$h = (2A(C_1 - C_2)Dt)^{1/2} \qquad (7)$$

By measuring h at several different times at a given temperature, and plotting h vs. $t^{1/2}$, one can obtain a value of $K = 2A(C_1 - C_2)D$ at that temperature. An activation energy can be obtained by an Arrhenius plot of K as a function of inverse temperature in Kelvins, based on the expression

$$K = K_0\exp(-Q/RT) \qquad (8)$$

When the parameters K_0 and Q have been found, the growth of a layer over time can be estimated. Equation (7) can be transformed to

$$2h\frac{dh}{dt} = K_0\exp(-Q/RT) \qquad (9)$$

and by using the temperatures described in equations (3) and (4) this can be integrated (numerically)

$$h^2 = \int_0^t K_0 \exp(-\frac{Q}{RT(t)})dt \qquad (10)$$

to give the predicted layer thicknesses.

Unfortunately for the purposes of prediction, the exposure experiments in this study did not reveal a region of parabolic growth behavior. Instead, they indicated that the reaction rate at the higher temperatures to which the cask is exposed in the first few years of exposure is so rapid that the thickness of the intermetallic layer would soon become limited by the supply of zinc.

The thickness of the intermetallic layers seen at 30 and 90 days at 400 °C indicate that, if an unlimited supply of zinc were available at this temperature, and if growth of the intermetallic is proportional to the square root of time, the entire wall of a Zircaloy-4 fuel rod tube would be transformed to intermetallic within less than a year at this temperature. However, the supply of zinc is not unlimited, and one can make a very rough estimate of the thickness of intermetallic expected if the zinc paint consists of a 1 mm thick layer of pure zinc. Considering a PWR assembly of 14x14 or 196 rods, about 21 cm square (Ref. 4), each Zircaloy fuel rod having a diameter of 1.1 cm, the surface area of the Zircaloy fuel rods is $1.1 \times \pi \times 196 = 677$ cm^2 per centimeter length of the assembly. If this is enclosed in a square steel enclosure 21 cm on a side, the surface area of the steel enclosure is 84 cm^2 per unit length of the assembly. If the enclosure is coated with zinc paint to a thickness of 0.1 cm, and all of this zinc is distributed evenly on the Zircaloy fuel rods, the thickness of zinc on the fuel rods would be $0.1 \times 84/677 = 0.0124$ cm, or 124 μm. If this zinc were to react with the Zircaloy to eventually form the most zirconium rich intermetallic compound, ZnZr, the thickness of the reaction layer would be roughly 250 μm, or approximately 1/3 the thickness of the wall of the Zircaloy tubes. Numerous factors, however, could alter this thickness. The thickness of the reaction layer would probably be larger on tubes near the outside of the bundle and smaller on tubes in the interior of the bundle. Much of the zinc could be transported to the cooler exterior wall of the cask, far from the zircaloy surface. In fact, the temperatures shown at short times for the cladding are well above the melting point of zinc, so that if the zinc layer is as thick as 1 mm, much of it may melt and run to the bottom of the cask. An effort to estimate these effects was beyond the scope of the present study, which measured the reaction rates under isothermal conditions within a confined volume.

6.2 Mechanical Behavior

The C-bend tests were carried out at room temperature to detect severe embrittlement. As noted in the results section, the exposed and unexposed tests all failed by plastic collapse. Despite the presence of a brittle intermetallic layer on the surface of the exposed samples, the remaining, unreacted Zircaloy kept the C-ring from breaking in the elastic range. Since the stress analysis for this geometry is only available in the elastic range (ASTM Standard Test Method C1323-96), the outer fiber stress at the onset of plasticity was determined from the load-displacement curves. This flow stress is

plotted against zinc-exposure conditions in Figure 9. From this curve, it is clear that the more severe the exposure conditions, the greater the reduction in apparent flow stress. Given the behavior of the samples, it is clear in retrospect that the C-bend test is not a good method of characterizing the mechanical effect of zinc exposure due to the amount of plasticity prior to failure. However, they did rule out the presence of a glass-like brittleness resulting from zinc exposure under the conditions studied here.

Tensile tests on tubes provided information on the strength, ductility, and fracture mechanisms at slow strain rates and elevated temperatures. These results were not limited by the plastic deformation that took place prior to fracture. The exposure to zinc led to reductions in both strength and ductility as shown in Figures 10 and 11.

The loss in strength was related to the severity of exposure to zinc. The 90 day exposures at 350 °C and 400 °C caused nearly identical strength reductions. The exposure for 30 days at 650 °C was much more severe in this regard. It is also possible that there was some reduction in the strength of the Zircaloy due to the prolonged thermal exposure. An attempt was made to estimate the effect of the layer by calculating the UTS assuming that the load was born only by the remaining Zircaloy. The results of these calculations are shown in Figure 12 and were conservative for the 350 °C and 400 °C exposures, but non-conservative for the 650 °C exposures. Nevertheless, the results were reasonably good and suggest that the thicker the layers, the greater the reduction in strength. This has the clear implication that increasing the exposure to zinc will result in thicker layers and greater strength reductions.

The reductions in ductility are more complex. For all exposed conditions, the ductility reductions from the unexposed condition are approximately equal at a testing temperature of 350 °C. At a testing temperature of 100 °C, the sample exposed to zinc for 30 days at 650 °C has a ductility between that of no exposure and the other exposure conditions. Considering the fact that only one sample was tested at each condition, it is possible that this datum represents an atypical result and does not justify an explanation at this time. It is clear that significant ductility reductions resulted from the exposures studied here and should be expected in actual situations. However, the magnitude of such ductility reductions in thicker deposits cannot be determined from the present research.

Fractography (Figure 7) revealed that the intermetallic always cleaved and that the Zircaloy always failed by fibrous fracture under the conditions studied here. Figure 8 is an example of extensive cracking of the intermetallic layer due to the deformation of the underlying Zircaloy. This degree of cracking suggests that the intermetallic supported no load by the strain level associated with the UTS. However, the layers formed at 350 °C and 400 °C were adherent. They could have constrained deformation of the substrate material resulting in some strengthening as noted in the layer-corrected UTS, Figure 12. The adherent layer may also tend to localize the deformation to the cracked areas. Significant amounts of the intermetallic layers on the

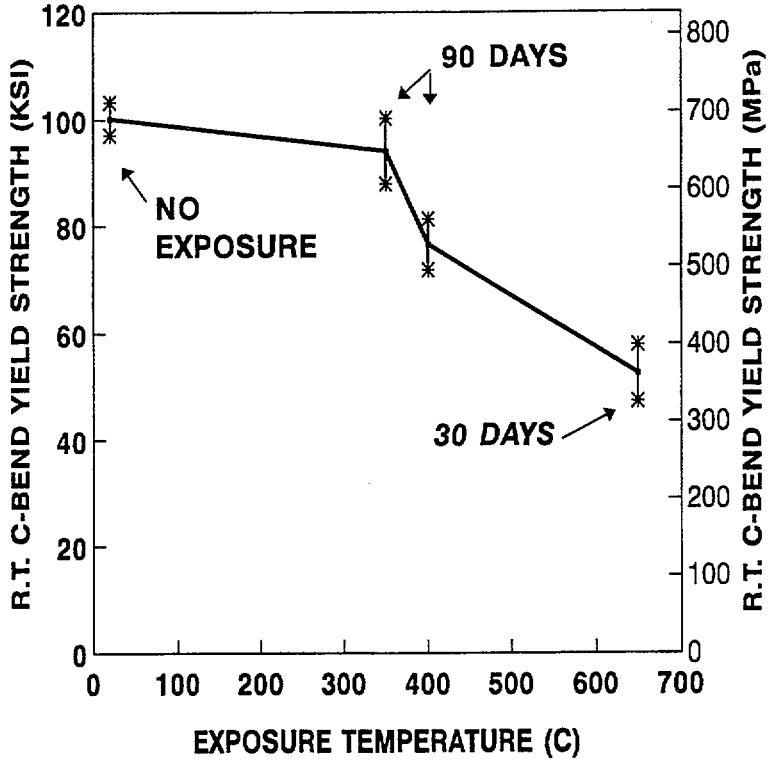

Figure 9 Effect of exposure conditions on the onset of plasticity as detected by the C-bend test at room temperature.

samples exposed to zinc at 650 °C flaked off during testing at 100 °C. This may be responsible for some of the ductility differences in the exposed material.

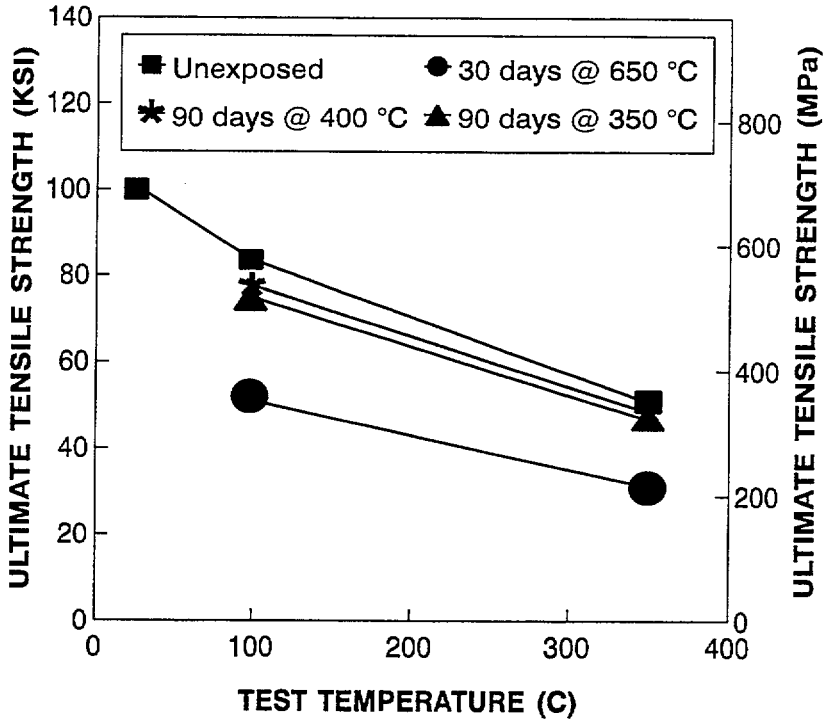

Figure 10 Effect of exposure condition on the slow strain rate ultimate tensile strength of Zircaloy tubes tested at the temperatures indicated.

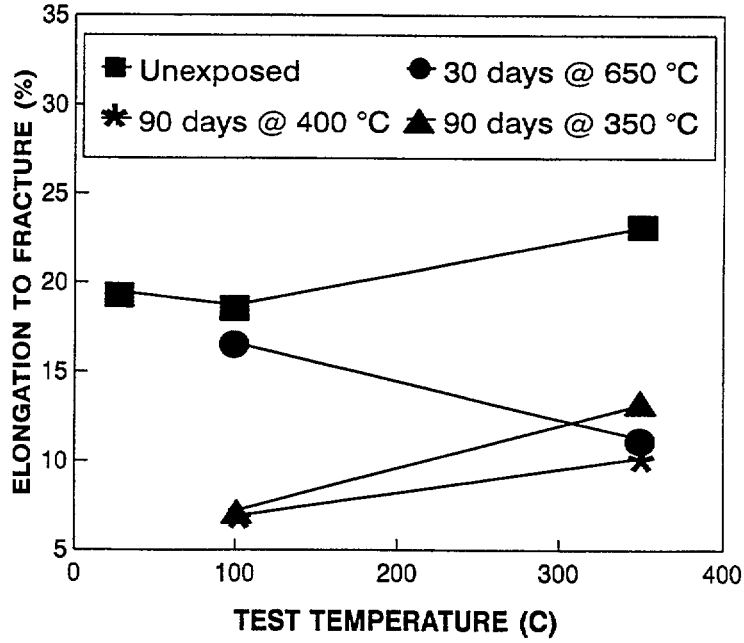

Figure 11 Effect of exposure conditions on the ductility of Zircaloy tubes tested in slow strain at the temperatures shown.

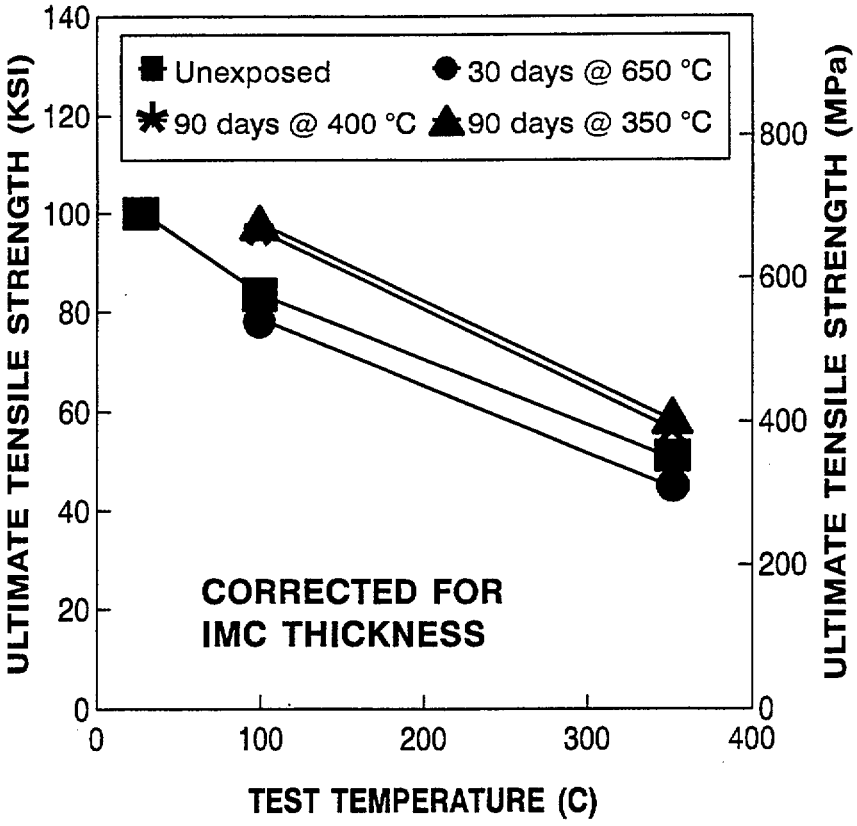

Figure 12 Assuming that the IMC layer is not load bearing, the UTS of the remaining Zircaloy is recalculated using the measured thickness of intermetallic and its stoichiometry.

7 CONCLUSIONS

The reaction between zinc vapor and Zircaloy-4 in the temperature range 300 °C to 400 °C is strongly dependent on temperature and probably on other as yet unidentified factors relating to the condition of the Zircaloy surface. At the low end of this temperature range, a few minute particle of Zn_3Zr were observed after the longest exposure time, but the observations were not sufficient to develop a credible model for the reaction rate at this temperature. At 350 °C, significantly larger and more abundant nodules of Zn_3Zr were formed, but their size and distribution did not vary in a systematic way with exposure time. This implied that the reaction at this temperature was strongly sensitive to the detailed condition of the sample surface, as would be expected for a nucleation and growth process. However, at 400 °C, the reaction was very different, and occurred by a uniform reaction mechanism much more rapid than the nodular growth observed at the lower temperatures.

The reaction of zinc with bare Zircaloy-4 at 400 °C was so rapid that it would quickly consume the entire wall of a fuel rod, if the supply of zinc were unlimited. Numerous factors could limit the supply of zinc to the Zircaloy surface, including movement of zinc from the paint to other regions of the storage cask. No attempt was made, however, to quantify such movements.

The oxide coating on EOL Zircaloy-4 tubes was found to be effective at reducing the rate of reaction of zinc vapor with the underlying Zircaloy, even though the oxide showed numerous cracks which would have facilitated its penetration by zinc vapor. The reaction was much more rapid at or near regions where the oxide coating was removed, and the potential exists for penetration of the Zircaloy in such regions. Any prediction of the long-term behavior of Zircaloy-4 clad fuel rods in a storage cask that has been coated with zinc paint would have to be made on the basis of measurements or analysis of supply, transport, and redistribution of zinc within the cask. An intact coating of oxide on the fuel rods can significantly reduce the rate of reaction of the zinc vapor with the fuel rods, perhaps providing sufficient time for the zinc to move elsewhere in the container.

C-bend and tensile tests were performed on Zircaloy tubing. Compared to as-received tubing, significant reductions in strength and ductility were associated with exposure to zinc at elevated temperatures. The strength reductions were correlated with the thickness of the intermetallic layer that formed. The ductility reductions due to exposure were related to the layer thickness in a more complex way. Unreacted Zircaloy always exhibited a fibrous fracture surface for all conditions of exposure to zinc. The intermetallic compounds that formed always exhibited a cleavage fracture surface.

REFERENCES

1. Manning, J. R., and Williams, M. E., "Reactions of Zinc Vapor with Zircaloy," report to Nuclear Regulatory Commission on FFS Commitment AA7500015, July, 1998.

2. Handbook of Chemistry and Physics, *Vapor Pressure Variation with Temperature,* CRC Press, 65th ed., 1985, p. D-215.

3. Safety Analysis Report, VSC-24 Cask SS, by Pacific Sierra Nuclear Associates and Sierra Nuclear Corp., December 1993.

4. "Onsite Storage of Spent Nuclear Fuel", http://www.nrc.gov/OPA/drycask/spntfuel.htm

NRC FORM 335 (2-89) NRCM 1102, 3201, 3202

U.S. NUCLEAR REGULATORY COMMISSION

BIBLIOGRAPHIC DATA SHEET

(See instructions on the reverse)

1. REPORT NUMBER (Assigned by NRC, Add Vol., Supp., Rev., and Addendum Numbers, if any.)

NUREG/CR-6675

2. TITLE AND SUBTITLE

Interaction of Zinc Vapor with Zircaloy and the Effect of Zinc Vapor on the Mechanical Properties of Zircaloy

3. DATE REPORT PUBLISHED

MONTH	YEAR
June	2000

4. FIN OR GRANT NUMBER

Y6212

5. AUTHOR(S)

R.J. Schaefer, R.J. Fields, M.E. Williams

6. TYPE OF REPORT

Technical

7. PERIOD COVERED *(Inclusive Dates)*

8. PERFORMING ORGANIZATION - NAME AND ADDRESS *(If NRC, provide Division, Office or Region, U.S. Nuclear Regulatory Commission, and mailing address; if contractor, provide name and mailing address.)*

National Institute of Standards and Technology
Gaithersburg, MD 20899

9. SPONSORING ORGANIZATION - NAME AND ADDRESS *(If NRC, type "Same as above"; if contractor, provide NRC Division, Office or Region, U.S. Nuclear Regulatory Commission, and mailing address.)*

Division of Engineering Technology
Office of Nuclear Regulatory Research
U.S. Nuclear Regulatory Commission
Washington, DC 20555-0001

10. SUPPLEMENTARY NOTES

C. Santos, Jr., NRC Project Manager

11. ABSTRACT *(200 words or less)*

Spent fuel rods removed from reactor cores are loaded under water into steel casks, which are then removed from the water, vacuum dried, and welded closed for dry storage. In some cases, the inside of the steel casks has been coated with zinc paint to prevent corrosion during the under-water phase of this process, and concern has arisen that the zinc could react with the Zircaloy-4 cladding of the spent fuel, possible leading to decreased mechanical strength. This project investigated the kinetics of the reaction between Zircaloy-4 and zinc vapor, and the mechanical properties of Zircaloy-4 which had been exposed to zinc vapor.

12. KEY WORDS/DESCRIPTORS *(List words or phrases that will assist researchers in locating the report.)*

Zircaloy, zinc, mechanical properties, intemetallic phases, reaction rates

13. AVAILABILITY STATEMENT

unlimited

14. SECURITY CLASSIFICATION

(This Page) unclassified

(This Report) unclassified

15. NUMBER OF PAGES

16. PRICE

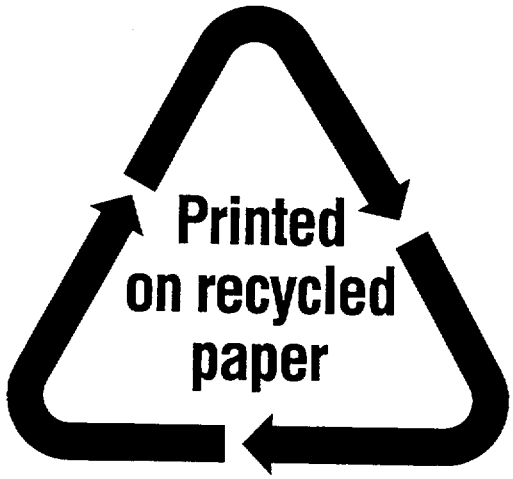

Federal Recycling Program

UNITED STATES
NUCLEAR REGULATORY COMMISSION
WASHINGTON, D.C. 20555-0001